Cell Stem Cell
Article

Cdk4/CyclinD1 Overexpression in Neural Stem Cells Shortens G1, Delays Neurogenesis, and Promotes the Generation and Expansion of Basal Progenitors

Christian Lange,[1] Wieland B. Huttner,[2] and Federico Calegari[1,*]
[1]DFG-Research Center and Cluster of Excellence for Regenerative Therapies Dresden (CRTD), Medical Faculty, Technische Universität Dresden c/o Max Planck Institute of Molecular Cell Biology and Genetics, Pfotenhauerstr. 108, 01307 Dresden, Germany
[2]Max Planck Institute of Molecular Cell Biology and Genetics, Pfotenhauerstr. 108, 01307 Dresden, Germany
*Correspondence: federico.calegari@crt-dresden.de
DOI 10.1016/j.stem.2009.05.026

SUMMARY

During mouse embryonic development, neural progenitors lengthen the G1 phase of the cell cycle and this has been suggested to be a cause, rather than a consequence, of neurogenesis. To investigate whether G1 lengthening alone may cause the switch of cortical progenitors from proliferation to neurogenesis, we manipulated the expression of cdk/cyclin complexes and found that cdk4/cyclinD1 overexpression prevents G1 lengthening without affecting cell growth, cleavage plane, or cell cycle synchrony with interkinetic nuclear migration. Specifically, overexpression of cdk4/cyclinD1 inhibited neurogenesis while increasing the generation and expansion of basal (intermediate) progenitors, resulting in a thicker subventricular zone and larger surface area of the postnatal cortex originating from cdk4/cyclinD1-transfected progenitors. Conversely, lengthening of G1 by cdk4/cyclinD1-RNAi displayed the opposite effects. Thus, G1 lengthening is necessary and sufficient to switch neural progenitors to neurogenesis, and overexpression of cdk4/cyclinD1 can be used to increase progenitor expansion and, perhaps, cortical surface area.

INTRODUCTION

During mouse embryonic development, an increasing proportion of neural progenitors switch from divisions that generate two progenitors (proliferative divisions) to divisions that generate at least one neuron (neurogenic divisions). Specifically, with the onset of telencephalic neurogenesis at embryonic day 11 (E11), neuroepithelial cells forming the ventricular zone (VZ) start to switch from symmetric proliferative to asymmetric neurogenic division (Caviness et al., 1995; McConnell, 1995; Rakic, 1995). In addition, neuroepithelial and, later in development, radial glial cells, here referred together as apical progenitors (APs), asymmetrically generate a second progenitor type, the basal (or intermediate) progenitor (BP), that at mid-corticogenesis (E14) becomes the predominant neurogenic cell type (Haubensak et al., 2004; Miyata et al., 2004; Noctor et al., 2004). BPs lose polarity, migrate basally to form the subventricular zone (SVZ), and, in contrast to APs, undergo symmetric divisions that are only either proliferative or neurogenic (Attardo et al., 2008; Noctor et al., 2008). Importantly, the temporal and spatial control of the switch from proliferation to asymmetric and later symmetric neurogenesis regulates the balance between expansion, self-renewal, and consumption of the progenitor pool, ultimately establishing the size of the adult brain (Götz and Huttner, 2005; Kriegstein et al., 2006; Pontious et al., 2008).

Key to understand the mechanisms controlling the expansion versus differentiation of neural progenitors is the study of their cell cycle regulation (Bally-Cuif and Hammerschmidt, 2003; Dehay and Kennedy, 2007; Ohnuma and Harris, 2003). In particular, in respect to their cell cycle *length*, it has been observed that G1 increases as development proceeds (Takahashi et al., 1995) and that cortical regions with a higher proportion of neurogenic divisions are characterized by progenitors with a longer G1 (Lukaszewicz et al., 2005). Finally, population analyses have shown that at any given stage of development, neurogenic progenitors are characterized by a longer G1 than coexisting proliferative progenitors (Calegari et al., 2005).

In fact, several groups have reported a tight correlation between inhibition of cell cycle and neurogenesis showing, for example, that (1) cell cycle inhibitors are markers of neurogenic progenitors (Georgopoulou et al., 2006; Iacopetti et al., 1999), (2) overexpression (or knockout) of antiproliferative genes promotes (or inhibits) neurogenesis (Canzoniere et al., 2004; Ohnuma et al., 1999; Politis et al., 2007; Regad et al., 2009), and (3) secreted factors that inhibit cell cycle induce neurogenesis whereas, conversely, factors promoting cell cycle decrease it (Hodge et al., 2004; Lukaszewicz et al., 2002).

This correlation being evident, the fundamental question remains as to whether lengthening of the cell cycle is a *cause* or, alternatively, a *consequence* of neurogenesis. Remarkably, despite major efforts, the answer to this question remains elusive because most studies focused on trophic or transcription factors that, in addition to the cell cycle, may as well influence differentiation as also shown for cell cycle inhibitors such as $p27^{kip1}$ (Nguyen et al., 2006).

In support to a causal role of cell cycle length on neurogenesis, it has been observed that lengthening of G1 by inhibition of the cdk2/cyclinE1 complex, whose only characterized function is to control cell cycle progression, is sufficient to trigger premature

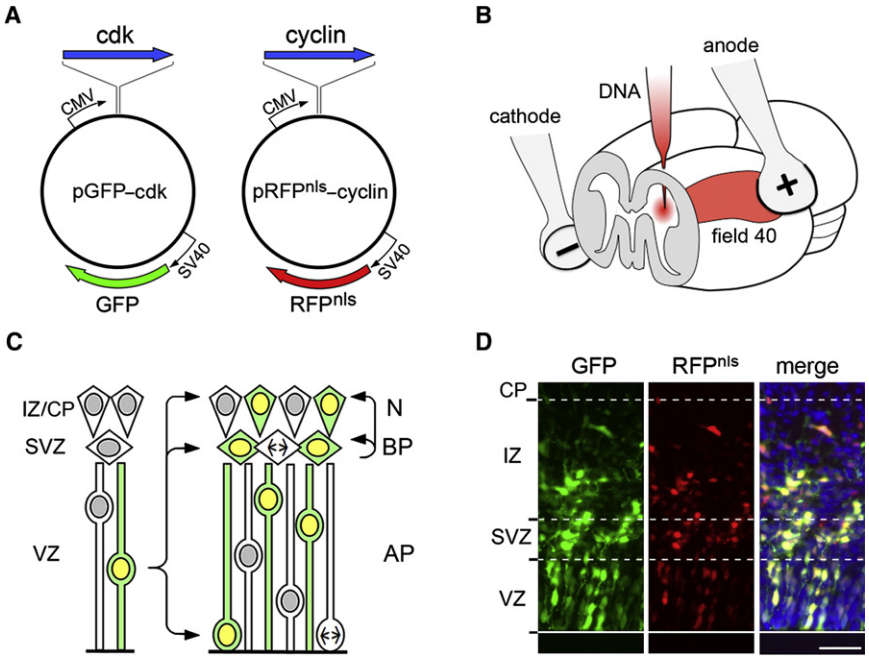

Figure 1. Experimental Approach

(A) Scheme of GFP (left) and RFPnls (right) vectors for cdk or cyclin, respectively. Note the use of similarly strong promoters for reporters (SV40) and cell cycle regulators (CMV).

(B) Drawing of the mouse brain in the rostral-left, caudal-right orientation after sectioning at the level of field 40 and removal of the rostral part. Positioning of the electrodes and DNA injection are indicated.

(C) Drawing exemplifying the cytoarchitecture of the developing brain with (1) bipolar APs in the VZ (bottom), (2) multipolar BPs (rhombuses) in the SVZ (middle), and neurons (deltoids) in the IZ/CP (top). Left and right represent the cortex either soon or few days after electroporation with GFP (green) and RFPnls (yellow, as merge with green) plasmids. Note the change in distribution of green/yellow cells from the VZ (left) to the VZ, SVZ, and IZ/CP (right) resulting from division of transfected progenitors (arrows). Pial endfeet of radial glia are not portrayed for clarity.

(D) Fluorescence pictures of a mouse brain 24 hr after electroporation at E13.5 with control plasmids showing the distribution of fluorescent cells in the VZ, SVZ, and IZ (dashed lines indicate boundaries of each). Note the almost complete colocalization of the reporters (merge; including DAPI) (white line, apical surface; scale bar represents 50 μm).

neurogenesis (Calegari and Huttner, 2003). Thus, a model was proposed, referred to as the cell cycle length hypothesis, according to which a cell fate determinant(s) may, or may not, induce a cell fate change of neural progenitors depending on whether or not the length of G1 provides enough time for the cell fate determinant-produced effect(s) to become effective. In essence, time may be a key limiting factor for cell fate change to occur and a relatively long G1 may allow the switch to neurogenesis while a short G1 may not (Calegari and Huttner, 2003).

However, validation of this hypothesis still awaits demonstration that shortening G1 prevents neurogenesis while increasing proliferative divisions. Importantly, in contrast to studies reporting induction of neurogenesis and depletion of the progenitor pool, a delay of neurogenesis should allow greater progenitor expansion resulting in increased brain size.

To address these possibilities, we manipulated the expression of genes whose only characterized function is to promote G1 or G1-to-S transition, e.g., the cdk4/cyclinD1 and cdk2/cyclinE1 complexes (referred to as 4D and 2E), respectively (Ekholm and Reed, 2000; Sherr, 1994), and investigated the effect of this manipulation on cell cycle length and cell fate change of neural progenitors during mouse corticogenesis.

RESULTS

Experimental Approach

To overexpress 4D or 2E and directly identify cdk/cyclin-overexpressing cells, we cloned cdk4 or cdk2 into a vector also encoding for GFP, and cyclinD1 or cyclinE1 into a vector also encoding for RFP (Figure 1A). Cytoplasmic GFP and a nuclear-localized RFP (RFPnls) were used to simultaneously identify shape and nuclei of transfected cells, which are important parameters to distinguish the boundary between the VZ and the SVZ by their different cytoarchitecture (Figures 1C and 1D) and to count cells reliably.

Immunofluorescence and western blot analyses on HeLa cells revealed that each cell cycle regulator was coexpressed with its fluorescent reporter and could form catalytically active complexes that triggered hyperphosphorylation of retinoblastoma, a primary target of G1-cdk/cyclins (Supplemental Data and Figure S1 available online). When electroporated in the E13.5 lateral cortex (Figure 1B), both GFP/RFPnls (referred to as control) and cdk/cyclin plasmids showed 24 hr later an almost complete (>95%) coexpression in transfected cells (Figure 1D).

Importantly, reproducibility of the region and number of cells transfected by in utero electroporation is limited. Thus, we analyzed only brains targeted in field 40 of the dorso-lateral cortex (Figure 1B) because of its ease of transfection and extensive characterization with regard to cell cycle length and cell fate change of neural progenitors and expressed numbers of targeted cells in each cortical zone, i.e., VZ, SVZ, intermediate zone (IZ), and cortical plate (CP), as a percentage of all transfected cells, which allows to quantify differentiation and neuronal output of a pool of targeted progenitors as a function of time (Figure 1C, left versus right; additional details in Supplemental Data).

Overexpression of 4D, but Not 2E, Shortens G1

To investigate whether overexpression of 4D or 2E accelerates the cell cycle of cortical progenitors, we electroporated E13.5 embryos with either (1) control, (2) 4D, or (3) 2E plasmids followed 24 hr later by cumulative BrdU labeling (Takahashi et al., 1995) and quantification of $BrdU^+$ cells in the VZ (Figures 2A and 2B).

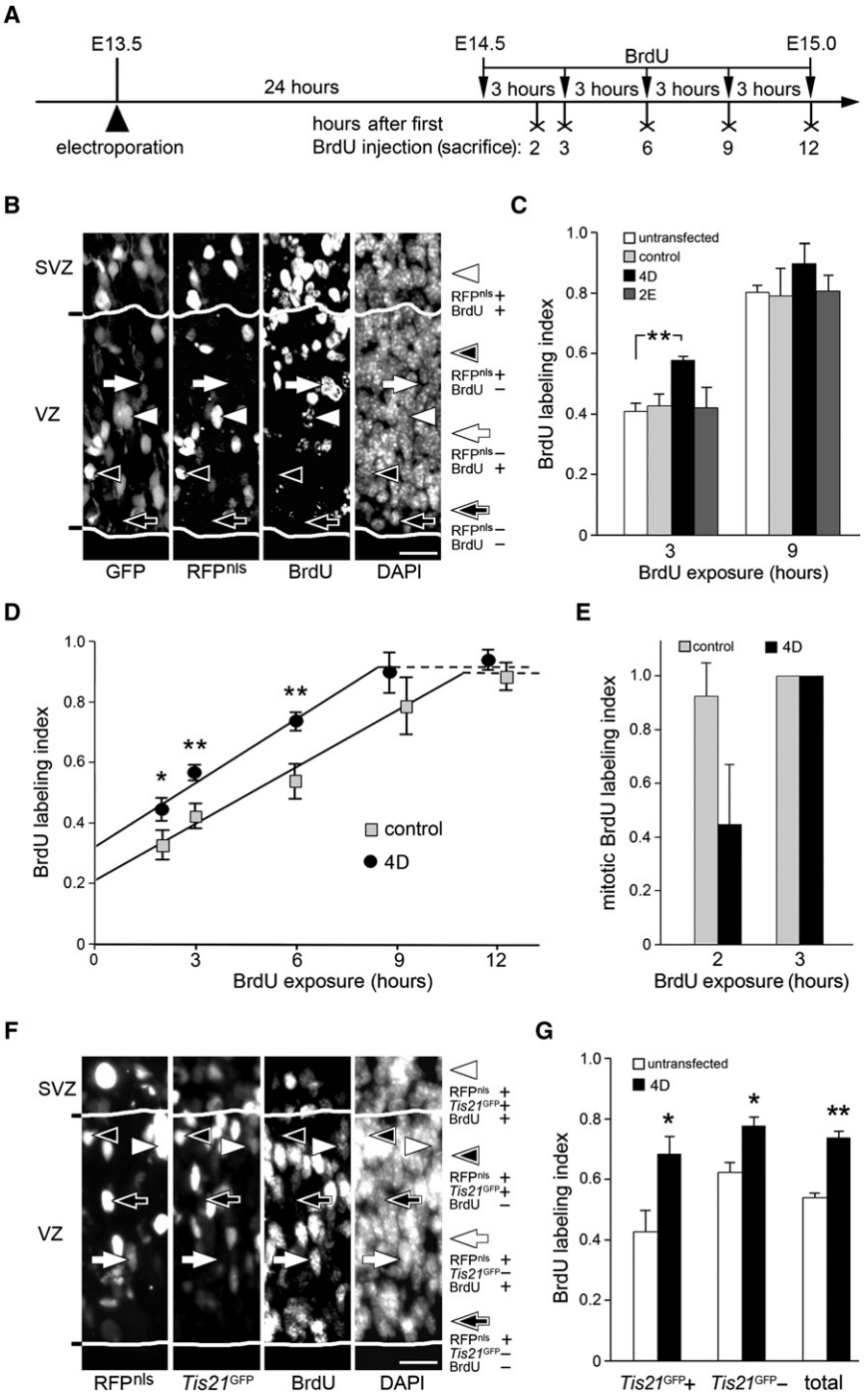

Figure 2. Cell Cycle Length Analyses

(A) Time course of cumulative BrdU labeling with electroporation performed at E13.5 (left; arrowhead) and BrdU injections (arrows) starting at E14.5 with 3 hr intervals. Mice were sacrificed 2, 3, 6, 9, or 12 hr after the first BrdU injection (crosses).

(B) Fluorescence pictures of a 2-μm-thick confocal optical section of the VZ and SVZ after electroporation with control plasmids and 2 hr BrdU exposure indicating RFPnls$^+$ (arrowheads) and RFPnls$^-$ (arrows) nuclei being scores as BrdU$^+$ (white arrowheads and arrows) or BrdU$^-$ (black arrowheads and arrows).

(C) BrdU labeling indices of VZ, untransfected cells (white), or cells transfected with control (light gray), 4D (black), or 2E (dark gray) plasmids after 3 (left) or 9 (right) hr BrdU exposure.

(D) Cumulative BrdU labeling curves of control (gray squares) or 4D-transfected (black circles) cells. Dashed lines indicate growth fractions.

(E) Mitotic BrdU labeling indices of control (gray) or 4D-transfected (black) cells after 2 (left) or 3 (right) hr BrdU exposure.

(F) Fluorescence pictures as in (B) of a *Tis21*^{GFP} embryo electroporated with GFP-lacking 4D plasmids followed by 6 hr BrdU exposure showing RFPnls$^+$/Tis21$^+$ (arrowheads) or RFPnls$^+$/Tis21$^-$ (arrows) nuclei being scored as BrdU$^+$ (white) or BrdU$^-$ (black).

(G) 6 hr BrdU labeling indices of untransfected (white) or 4D-transfected (black) cells among Tis21$^+$ (left) or Tis21$^-$ (middle) cells or being pulled together (total; right). Note the higher effect in the Tis21$^+$ than in the Tis21$^-$ population.

Lines in (B) and (F) indicate boundaries of the VZ. Scale bars represent 20 μm.

(C–E and G) Labeling index 1.0 = all nuclei stained. Data are the mean of three (12 hr: two) litters; error bars indicate SD (12 hr: SEM); cells counted in (D): 6858; *p < 0.05; **p < 0.005.

We first measured the percentage of BrdU$^+$ cells (referred to as BrdU labeling index, with an index of 1.0 being equivalent to 100% of labeled cells) at 3 and 9 hr, which were found to be essentially identical in untransfected or control transfected cells (0.41 ± 0.02 versus 0.42 ± 0.04 at 3 hr and 0.80 ± 0.02 versus 0.78 ± 0.09 at 9 hr, respectively; Figure 2C). These values are similar to previous studies on unmanipulated embryos (Calegari et al., 2005; Takahashi et al., 1995), indicating that neither electroporation nor GFP/RFPnls expression affect the cell cycle of neural progenitors.

In contrast, a higher proportion of 4D-transfected cells had incorporated BrdU at 3 (0.56 ± 0.02) and 9 (0.89 ± 0.07) hr (Figure 2C). In particular, the labeling index at 9 hr almost reached 1.0, suggesting labeling of the entire population of cycling cells already before 9 hr. In contrast, the labeling indices of 2E-transfected cells were indistinguishable from controls after 3 (0.42 ± 0.06) and 9 (0.80 ± 0.04) hr (Figure 2C), suggesting an acceleration of the cell cycle by 4D, but not 2E, overexpression.

To measure cell cycle phases after 4D overexpression, we combined cumulative and mitotic BrdU labeling index analyses, which allow us to calculate (1) S and total cell cycle length and (2) G2+M by the increase in BrdU labeling index as a function of time in interphase or mitotic cells, respectively (Takahashi et al., 1995). Cumulative BrdU labeling was performed for a total of 12 hr (Figures 2A and 2D), and mitotic cells at 2 and 3 hr (Figure 2E) were identified by chromatin

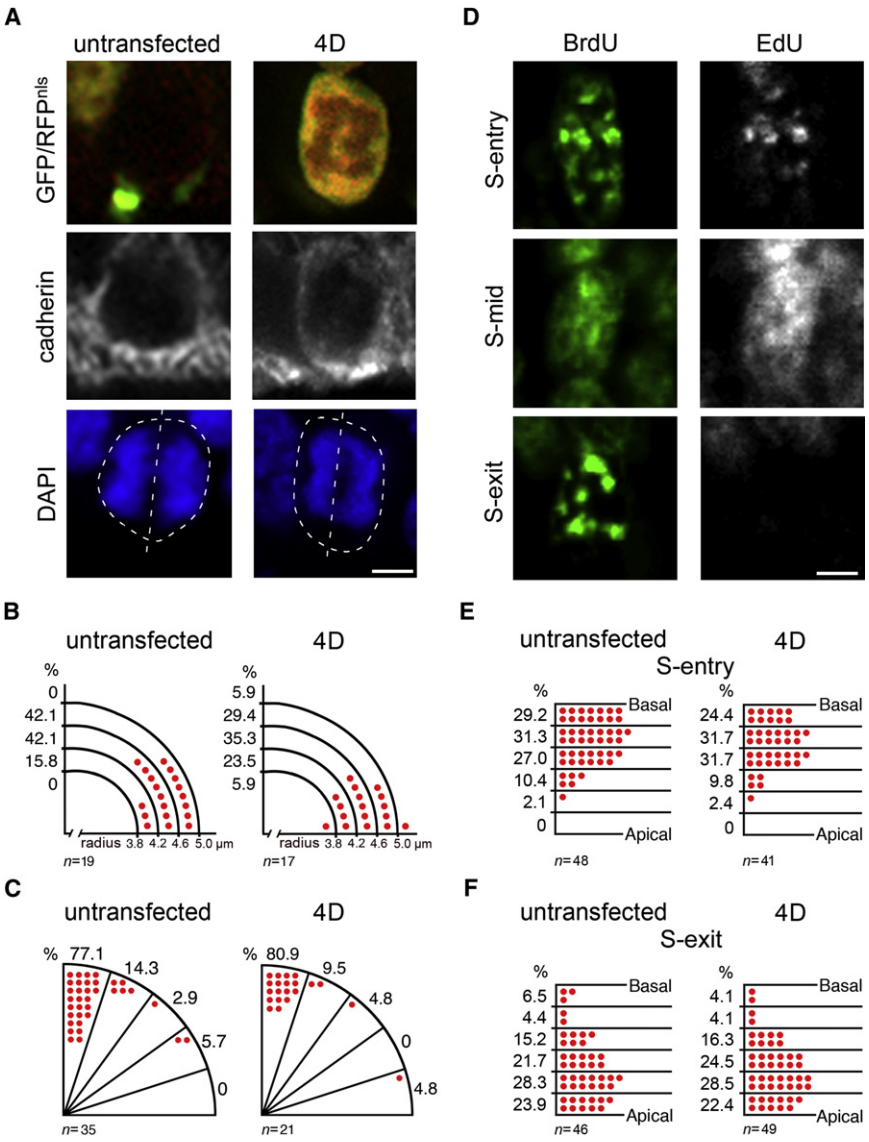

Figure 3. Analysis of Cell Size, Cleavage Plane Angle, and S Phase Entry or Exit

(A) Fluorescence pictures of 1-μm-thick confocal optical sections of untransfected (left) or 4D-transfected (right) mitotic AP after immunolabeling for cadherin (middle) and DAPI counterstaining (bottom). Dashed circles and lines (bottom) indicate the cadherin-outlined cell boundary and cleavage plane, respectively.

(B and C) Untransfected (left) or 4D-transfected (right) mitotic progenitors identified as in (A) were distributed in (1) five 0.4 μm intervals (from <3.4 to >5.0 μm) according to their radius (B) or (2) five 18° intervals according to their cleavage plane angle relative to the apical membrane (C).

(D) Fluorescence pictures of 2-μm-thick confocal optical sections through nuclei of progenitors exposed to BrdU for 90 min, with EdU being added during the last 45 min. Note the punctated versus homogeneous BrdU (left) and/or EdU (right) labeling indicating entry into (top), persistence through (middle), or exit from (bottom) S phase.

(E and F) Nuclei of untransfected (left) or 4D-transfected (right) progenitors entering (E) or exiting (F) S phase were distributed in six equidistant bins through the VZ.

Scale bars represent 3 μm.

condensation and diffusion of RFPnls to the cytoplasm (see example in Figure 3A).

We found that 4D-transfected progenitors had a 10% shorter cell cycle than control progenitors (13.1 versus 14.5 hr) (data given for 4D and control, respectively) and that the proportion of cycling cells was similar in both conditions (0.90 ± 0.03 versus 0.88 ± 0.05) (Figure 2D). It should be noticed that the effect of 4D on the total cell cycle occurred despite an increase of S by 35% (4.7 versus 3.5 hr) and of G2+M by 25% (2.5 versus 2.0 hr) (Figures 2D and 2E; Table S1). In fact, the G1 of 4D overexpressing progenitors was 30% shorter than that of control progenitors (5.9 versus 9.0 hr) (Table S1).

With the *Tis21*^{GFP} knockin mouse line, which allows us to identify neurogenic cells by the expression of GFPnls (Haubensak et al., 2004), it has been shown that proliferative Tis21$^-$ progenitors have a shorter G1 than neurogenic Tis21$^+$ progenitors (Calegari et al., 2005). Thus, to investigate whether 4D overexpression preferentially shortens the G1 of one progenitor subtype, we performed similar experiments in the *Tis21*^{GFP} line. E13.5 *Tis21*^{GFP} embryos were electroporated with GFP-lacking 4D plasmids and exposed to BrdU for 6 hr at E14.5. When BrdU incorporation was compared (Figure 2F), the increase in labeling index was more substantial among the Tis21$^+$ (60% increase) (0.42 ± 0.08 RFPnls$^-$ versus 0.68 ± 0.06 RFPnls$^+$) than the Tis21$^-$ (25% increase) (0.62 ± 0.03 RFPnls$^-$ versus 0.78 ± 0.03 RFPnls$^+$) population (Figure 2G), indicating a stronger effect of 4D overexpression on progenitors committed to lengthen G1.

Finally, for better understanding the molecular mechanism triggering the lengthening of G1 in neurogenic progenitors, or its shortening upon 4D overexpression, we investigated whether Tis21$^+$ progenitors specifically downregulated cyclinD1. Quantification of cyclinD1 immunoreactivity in nuclei of E14.5 Tis21$^-$ and Tis21$^+$ cells in the VZ revealed that this was the case because neurogenic progenitors displayed lower cyclinD1 immunoreactivity by 30% (Supplemental Data and Figure S2).

A Shorter G1 Does Not Affect Cell Growth, Cleavage Plane Angle, or Cell Cycle Synchrony with Interkinetic Nuclear Migration

Prior to studying the effect of 4D on neurogenesis, we considered it important to investigate whether a shorter G1 affects key features of neural progenitors, such as growth, cleavage plane angle, or interkinetic nuclear migration, parameters that may influence neurogenesis.

Thus, we electroporated E13.5 embryos with 4D plasmids, and 1 day (i.e., two cell cycles) later, we measured the size of targeted

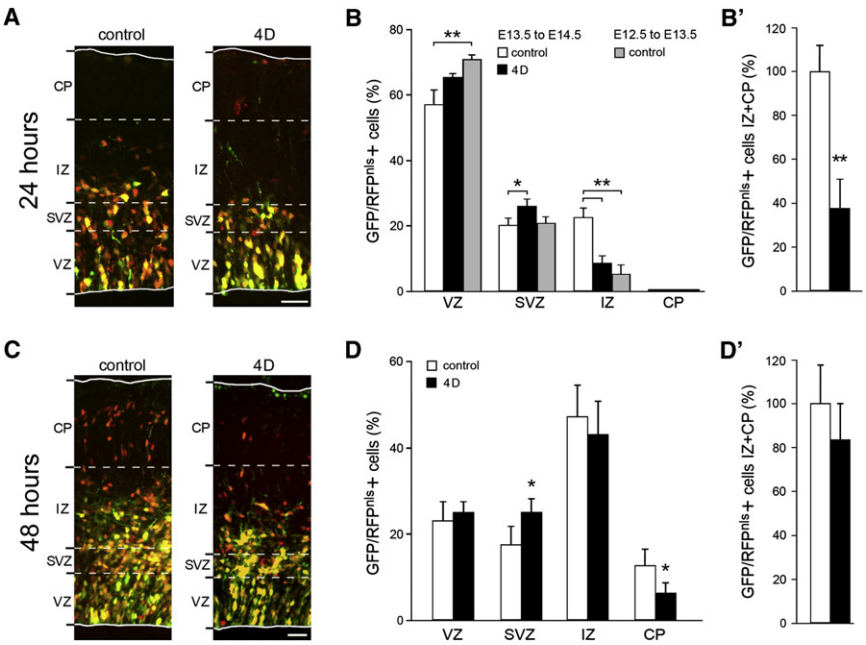

Figure 4. A Shorter G1 Inhibits Neurogenesis

(A and C) Fluorescence pictures of the mouse cortex after electroporation with control (left) or 4D (right) plasmids followed by 24 (A) or 48 (C) hr of development (GFP and RFPnls shown as merge) (DAPI and Tbr2 fluorescence not shown for clarity). Note the almost complete absence of fluorescent cells in the IZ at 24 hr and in the CP at 48 hr after electroporation with 4D. (Lines indicate apical and pial boundaries of the cortex; dashed lines indicate boundaries between cortical zones.) Scale bars indicate 50 μm.

(B, B′, D, and D′) Percentage of fluorescent cells in cortical zones 24 (B and B′) or 48 (D and D′) hr after electroporation with control (white; gray in B for electroporations at E12.5) or 4D (black) plasmids. (B′ and D′) Neuronal output calculated considering all IZ and CP fluorescent cells (control = 100%). Data are the mean of three litters; error bars indicate SD; cells counted: 12,574; *$p < 0.05$; **$p < 0.005$.

and coexisting, untransfected mitotic APs on consecutive optical sections (1 μm intervals) after immunolabeling for the membrane marker cadherin to define cell boundary (Figure 3A). This showed that a shorter G1 did not affect growth because, assuming a spherical shape, the radius of untransfected and 4D-targeted APs was essentially identical ($r = 4.55 \pm 0.31$ versus 4.46 ± 0.45 μm, respectively; ~380 fl volume) (Figures 3A and 3B). In addition, these analyses gave us the opportunity to measure cleavage plane angle of mitotic APs, which was also unaffected because most were vertical in either condition (Figure 3C).

Moreover, interkinetic nuclear migration is a hallmark of APs synchronizing cell cycle with nuclear movement. Nuclei of APs migrate basally during G1 and invert migration in S to undergo apical mitosis, so an artificially shorter G1 may induce S entry to occur closer to the apical surface.

To investigate this, we performed a 90 min BrdU labeling, with the BrdU analog EdU being added during the last 45 min, and analyzed BrdU/EdU incorporation in 4D-targeted and untransfected cells. In fact, a short (<30 min) exposure to the S-phase tracers results in a punctated labeling because of incorporation only at replication forks. Thus, we reasoned, equally punctated $BrdU^+/EdU^+$ staining will identify cells that have just entered S at the end of the double labeling whereas punctated $BrdU^+$, but EdU^-, nuclei will identify cells having left S during the first 30 min of BrdU exposure, i.e., 60 min prior to fixation (details in Supplemental Data and Figure S3; Figure 3D).

This revealed that the position of nuclei of 4D-overexpressing progenitors entering S or in the first hour of G2 was essentially identical to that of untransfected cells (Figures 3E and 3F), which suggests that a manipulation of the length of cell cycle phases induces a speeding up, or slowing down, of nuclear migration to maintain its synchrony with cell cycle progression.

Overexpression of 4D Inhibits Neurogenesis

Having excluded an effect of 4D on growth, cleavage plane angle, and interkinetic nuclear migration, we investigated whether shortening of G1 induced a cell fate change of neural progenitors, specifically, neurogenesis.

Embryos were electroporated with either control, 4D, or 2E plasmids at E13.5 and were collected 24 or 48 hr later. Boundaries between each cortical zone (i.e., VZ, SVZ, IZ, and CP) of the targeted area were identified on cryosections by (1) immunoreactivity for Tbr2, a marker of BPs and the SVZ (Englund et al., 2005), (2) morphology of GFP^+ cells, and (3) an abrupt increase in the density of DAPI-labeled nuclei between IZ and CP. Finally, $RFPnls^+$ nuclei in each zone were expressed as a percentage of all $RFPnls^+$ nuclei.

Analyses 24 hr after electroporation with control plasmids showed a distribution of $RFPnls^+$ cells in the VZ, SVZ, and IZ in line with the expected values at this developmental stage (58.1% ± 3.5%, 20.0% ± 2.4%, and 21.9% ± 2.5%, respectively). Also, no cell was observed in the CP, because neurons generated in the previous 24 hr presumably did not yet complete their migration toward it (Figures 4A and 4B).

In contrast, the proportion of $RFPnls^+$, 4D-targeted cells showed an increase by 10% and 30% in the VZ and SVZ with a reduction by 60% in the IZ (64.6% ± 0.4%, 26.4% ± 2.0%, 9.0% ± 2.0%, respectively) (Figures 4A, 4B, and 4B′). Interestingly, this distribution resembled that of the E13.5 cortex electroporated with control plasmids at E12.5 (71.5% ± 1.3%, 21.7% ± 1.8%, 6.7% ± 2.7% in the VZ, SVZ, and IZ, respectively) (Figure 4B), suggesting that 4D overexpression inhibits the switch from proliferation to neurogenesis between E13.5 and E14.5.

Electroporation with 2E plasmids showed a similar trend (60.2% ± 3.5%, 21.9% ± 3.1%, 17.9% ± 2.8% in the VZ, SVZ, and IZ, respectively) though the change was small and not significant (not shown). Thus, no further investigation on 2E was performed.

Importantly, the reduced proportion of $RFPnls^+$ cells in the IZ after 4D electroporation was not due to mortality of neurons nor to a defected migration. In fact, a similarly negligible number

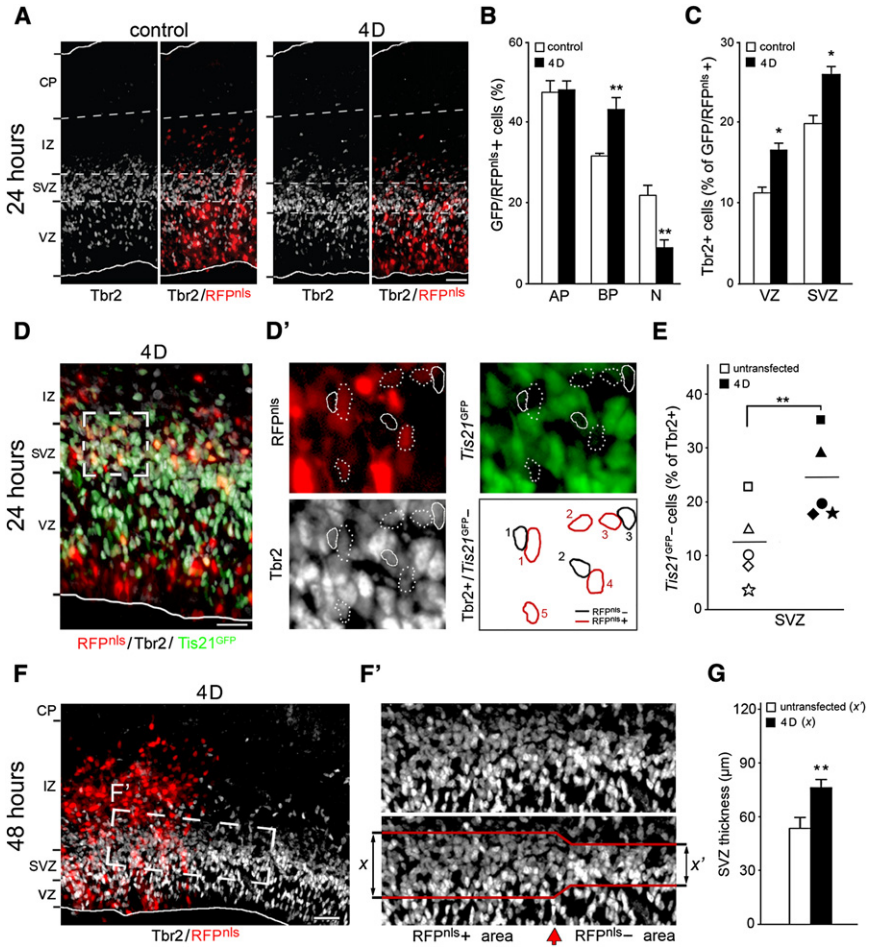

Figure 5. A Shorter G1 Increases the Generation and Expansion of BPs

(A) Fluorescence pictures of the mouse cortex after electroporation with control (left) or 4D (right) plasmids, 24 hr of development and Tbr2 immunoreactivity (white; merged with RFP).

(B) Quantification of APs, BPs, and neurons (N) as in (A).

(C) Quantification of Tbr2$^+$ cells and their distribution in the VZ or SVZ.

(D) Merged fluorescence pictures after electroporation of a *Tis21*^{GFP} embryo with GFP-lacking 4D plasmids and Tbr2 immunolabeling.

(D′) Magnification of the dashed box in (D) showing individual RFPnls, *Tis21*^{GFP}, and Tbr2 channels and Tbr2$^+$/Tis21$^-$ cells being scored in the RFPnls$^+$ (dotted lines) or RFPnls$^-$ (lines) population.

(E) Quantification of Tbr2$^+$/Tis21$^-$ cells in the SVZ. Each symbol represents quantification within the same optical field from five brains.

(F) Fluorescence pictures as in (A) but at 48 hr after electroporation with 4D plasmids.

(F′) Magnification of the dashed box in (F) showing individual Tbr2 staining (top) and the area being considered as SVZ (area between red lines; bottom). Note the abrupt increase in thickness of the SVZ (*x* versus *x*′) at the border of the RFPnls$^+$ area (red arrow).

(G) Quantification of the effect shown in (F′) for three cortices with ~50% electroporation efficiency.

(A, D, F) Lines indicate boundaries of the cortex; scale bars represent 50 μm. (A) Dashed lines indicate boundaries between cortical zones. Data are the mean of three litters (E: five embryos from three litters); error bars indicate SD; cells counted in (B) and (E): 3765 and 1065, respectively; *p < 0.05; **p < 0.005.

of apoptotic cells, identified by pycnotic nuclei or caspase-3 immunoreactivity, and β-III-tubulin$^+$ cells in the VZ or SVZ were found in cortices electroporated with control or 4D plasmids or in unelectroporated cortices (Figure S4 and data not shown). Thus, these experiments indicate that a shortening of G1 inhibits neurogenesis.

Additional experiments confirmed this conclusion. Electroporation followed by a longer survival time (48 hr), which allows migrating neurons to reach the CP, again showed a change in the proportion of cells in the VZ, SVZ, IZ, and CP after targeting with control (23.4% ± 4.3%, 17.3% ± 4.7%, 47.1% ± 7.8%, and 12.2% ± 3.4%, respectively) as compared to 4D (24.8% ± 2.9%, 25.0% ± 2.9%, 43.8% ± 7.2%, and 6.3% ± 2.6%, respectively) plasmids with a reduction of neurons in the IZ and CP by 20% and an increase in progenitors in the SVZ by 45% (Figures 4C, 4D, and 4D′).

In conclusion, shortening G1 by 4D overexpression inhibited neurogenesis and increased the proportion of progenitors in the SVZ (Figures 4B and 4D). Intriguingly, because most neurons are thought to be generated by BPs in the SVZ (Haubensak et al., 2004; Pontious et al., 2008), it may be expected that 48 hr after 4D overexpression, the proportion of neurons should be increased. Yet, this proportion was decreased (Figure 4D′), suggesting that shortening of G1 induces BPs to undergo proliferative rather than neurogenic division.

Overexpression of 4D Increases the Generation and Expansion of BPs

We then analyzed whether the increased proportion of progenitors at the expense of neurons was due to a cell fate change of APs, BPs, or both by analyzing the expression of the BP marker Tbr2 (Englund et al., 2005) in RFPnls$^+$ cells 24 hr after electroporation at E13.5 with either control or 4D plasmids (Figure 5A). Specifically, RFPnls$^+$ cells were divided in three groups: (1) Tbr2$^-$ cells in the VZ, (2) Tbr2$^+$ cells in the VZ or SVZ, and (3) Tbr2$^-$ cells in the SVZ and cells in the IZ or CP irrespective of Tbr2 expression, representing APs, BPs, and neurons, respectively.

The proportions of APs, BPs, and neurons after targeting with control (46.7% ± 2.7%, 31.4% ± 0.6%, and 21.9% ± 2.6%, respectively) or 4D plasmids (47.7% ± 2.2%, 43.3% ± 3.0%, 9.0% ± 2.1%, respectively) showed a similar amount of APs but an increase in BPs by 40% (Figure 5B). In addition, the increase in BPs was found to occur not only in the SVZ but also, and to a similar extent, in the VZ (Figure 5C), indicating an increased generation of BPs.

We then used the *Tis21*^{GFP} line and investigated whether a higher proportion of BPs in the SVZ underwent proliferative, rather than neurogenic, division upon 4D overexpression. The percentage of proliferating Tbr2$^+$/Tis21$^-$ BPs in the SVZ was calculated in the two subpopulations of RFPnls$^+$ and coexisting

RFPnls$^-$ cells 24 hr after electroporation of E13.5 *Tis21*^{GFP} mice with GFP-lacking 4D plasmids, which showed a 2-fold increase in the proportion of proliferating BPs in the RFPnls$^+$ population (24.3% ± 7.9% versus 12.4% ± 7.2%) (Figures 5D, 5D′, and 5E). Moreover, consistent with an increased expansion of BPs, 48 hr after electroporation with 4D, we found a 40% thickening of the SVZ containing RFPnls$^+$ BPs as compared to the adjacent SVZ within the same optical field (76.2 ± 2.9 versus 54.2 ± 5.3 μm, for the RFPnls$^+$ and RFPnls$^-$ area, respectively) (Figures 5F, 5F′, and 5G).

Finally, we investigated whether 4D overexpression may also influence the switch from neurogenesis to gliogenesis by electroporation at E15.5 (i.e., at the onset of gliogenesis) and analyses at E18.5 (i.e., 1 day after the end of cortical neurogenesis). After electroporation with control or 4D plasmids, expression of markers of radial glia (BLBP), proliferation (PCNA), or gliogenic transition (Olig2 and CD44) was determined. In brief, these experiments showed no change with regard to the (1) abundance and distribution of BLBP$^+$ or PCNA$^+$ cells, essentially all restricted to germinal zones, (2) proportion of Olig2$^+$ cells, and (3) premature expression of CD44, which was detected only postnatal (details in Supplemental Data), suggesting that 4D overexpression does not influence the switch from neurogenesis to gliogenesis.

4D RNAi Induces the Converse Effects of 4D Overexpression

Overexpression of 4D shortens G1, inhibits neurogenesis, and increases the generation and expansion of BPs, so we investigated whether 4D knockdown by RNAi via in utero electroporation (Calegari et al., 2004) induced the opposite effects.

Embryos were electroporated at E13.5 with two plasmids coexpressing GFP and a shRNA against either cdk4 (SA-Biosciences) or cyclinD1 (Peng et al., 2006) (referred to as 4- and D-shRNA, or 4D-shRNA if pulled together), which 48 hr after transfection reduced cdk4 levels by western blot analysis in NIH 3T3 by 60% (Figures 6A and 6B) and cyclinD1 immunoreactivity in the cortex by 40% (Figures 6C and 6D), respectively (details in Supplemental Data). Electroporation with 4D-shRNA and RFPnls plasmids was performed at E13.5 followed 48 hr later by quantification of BrdU$^+$ or Tbr2$^+$ cells and their distribution in cortical zones.

4D RNAi reduced BrdU labeling indices both at 3 and 9 hr (0.42 ± 0.05 versus 0.32 ± 0.02 at 3 hr and 0.72 ± 0.09 versus 0.57 ± 0.06 at 9 hr for untransfected and 4D-shRNA targeted cells, respectively) (Figure 6E) without a significant change in the proportion of cycling cells (0.92% ± 0.03% versus 0.87% ± 0.01%) (data not shown), suggesting a lengthening of G1 by 2.4 hr. Moreover, the 9 hr cumulative BrdU labeling was also used as neuronal birthdating experiment to measure the proportion of BrdU$^+$ neurons in the IZ generated from untransfected or 4D-shRNA-targeted progenitors during the 9 hr prior to sacrifice at E15.5, i.e., when an effect on G1 length could be ascertained (details in Supplemental Data). This revealed a 40% increase in neurons from 4D-shRNA-targeted progenitors as compared to untransfected progenitors (19.2% ± 3.3% versus 13.6% ± 3.9%, respectively) (Figure 6F) and thus induction of neurogenesis upon lengthening of G1.

Finally, APs and BPs in the VZ or SVZ were identified by Tbr2 and expressed as percentage of all progenitors 48 hr after electroporation at E13.5 with (1) control, (2) 4D, or (3) 4D-shRNA plasmids. This revealed that the effect of 4D overexpression was conversely mirrored by 4D RNAi (Figure 6G). Specifically, after 4D overexpression, APs, BPs in the VZ, or BPs in the SVZ had changed relative to control by −30%, +25%, and +15%, respectively (AP, 37.7% ± 2.6% versus 25.4% ± 5.3%; BP in the VZ, 23.9% ± 3.0% versus 29.8% ± 3.3%; BP in the SVZ, 38.4% ± 2.1% versus 44.8% ± 2.9% for control or 4D plasmids, respectively). (The decrease in APs at E15.5 is not in contradiction with their unchanged proportion at E14.5 [Figure 5B] because neurons are included in the latter but not in the former calculation.) Conversely, after 4D RNAi, APs, BPs in the VZ, and BPs in the SVZ had changed relative to control by +30%, −20%, and −20% (49.7% ± 6.0%, 19.7% ± 3.3%, and 30.6% ± 4.0%, respectively) (Figure 6G).

Altogether, conversely to 4D overexpression, 4D RNAi lengthens G1, induces neurogenesis, and inhibits the generation and expansion of BPs. Importantly, no effect by 4D-shRNA was observed with regard to (1) interkinetic nuclear migration (judged by the distribution of BrdU$^+$ cells), (2) cell size and shape (judged by the area and profile of GFP$^+$ cells), or (3) migration (judged by the distribution of cell types in cortical zones) (data not shown).

Neurons Generated by 4D-Targeted Progenitors Occupy a Wider Cortical Area

BPs are thought to be the major source of neurons in the cortex, and an increase in their proportion during evolution has been proposed to underlie cortical expansion (Abdel-Mannan et al., 2008; Fish et al., 2008; Kriegstein et al., 2006; Pontious et al., 2008).

We therefore investigated whether a higher generation and expansion of BPs correlated with an increased cortical surface area by electroporation at E13.5 with either control or 4D plasmids and analysis at birth (P0). However, a limitation of our method was the difficulty to directly measure the area of the VZ being originally targeted. As a feasible approach, we sought to retrospectively infer the size of the VZ targeted at E13.5 by measuring the area that at P0 still contained residual GFP/RFPnls$^+$ cells and to assume that this area would be a reliable indicator of that originally targeted. Thus, we performed serial consecutive vibratome sections (50 μm thick) through the entire rostral-to-caudal axis of the P0 brains and measured, in each of them, the surface area of the apical VZ and the pial CP that contained RFPnls$^+$ cells, regardless on their abundance (Figures 7A, 7B, and 7B′).

Individual electroporations with either control or 4D plasmids showed a high degree of variability with regard to apical and pial surface area containing RFPnls$^+$ cells (e.g., pial area control from 1 to 4 mm^2), which reflects the variable efficiency of this technique. Remarkably, however, when we sought to normalize for this variability and expressed the pial surface area as a proportion of the apical one, we observed that the ratio of pial-to-apical surface area was highly reproducible with a value of 6.3 ± 1.0 for control plasmids (Figure 7C), which is consistent with stereological analyses on unmanipulated brains (Popken et al., 2004) and, thus, suggests the suitability of our methodology.

Electroporations with 4D plasmids showed an increase in the ratio of pial-to-apical surface area from 6.3 ± 1.0 to 15.5 ± 3.3 (Figure 7C). Thus, progenitors transfected with 4D at E13.5

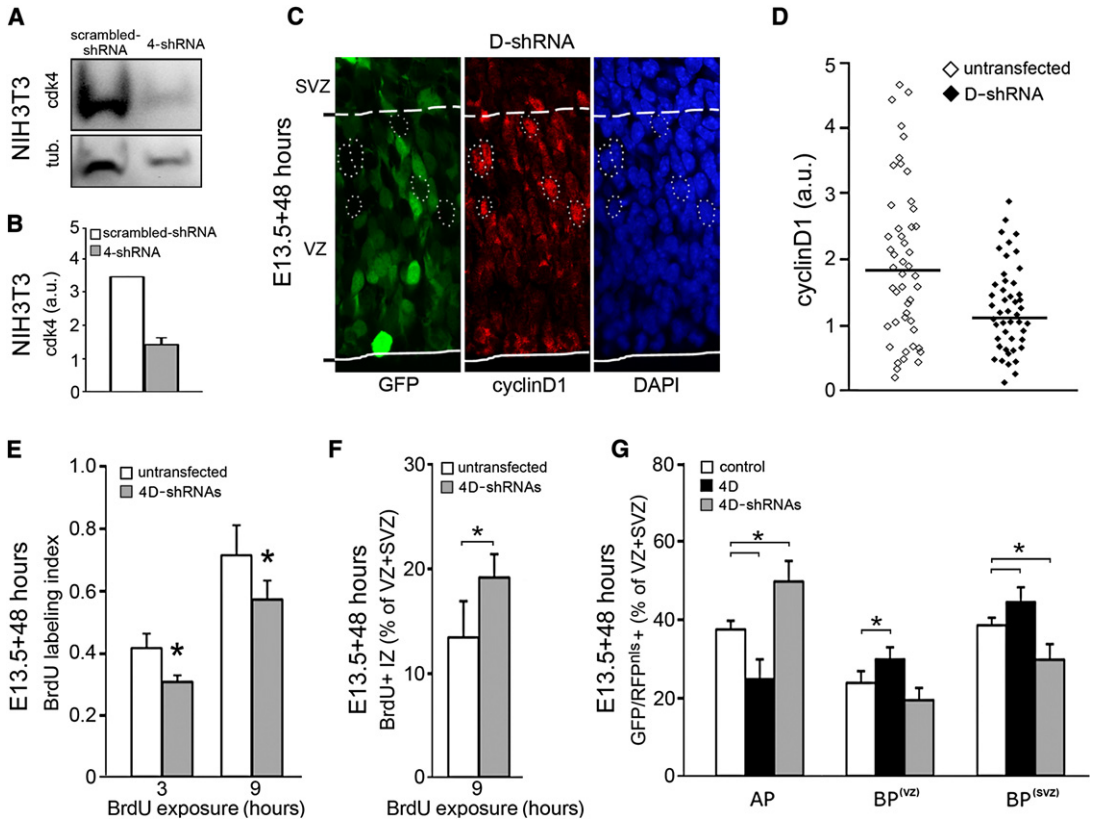

Figure 6. 4D RNAi Has the Converse Effect of 4D Overexpression

(A) Western blots for cdk4 and α-tubulin (tub.) 48 hr after transfection of NIH 3T3 with 4- or scrambled-shRNA and FAC sorting of GFP^+ cells.

(B) Quantification of cdk4 after tubulin normalization (3.5 = scrambled-shRNA; n = 2; error bars indicate SEM).

(C) Fluorescence pictures of the E15.5 VZ and SVZ after electroporation at E13.5 with D-shRNA, cyclinD1 immunolabeling, and DAPI staining. Note that high cyclinD1 immunoreactivity was found only within GFP progenitors (dotted circles) (continuous and dashed line indicate apical and basal boundary of the VZ, respectively).

(D) Quantification (a.u.) of cyclinD1 immunoreactivity in 48 GFP^- (white) or GFP^+ (black) nuclei randomly chosen within the VZ (bars indicate mean; $p < 0.05$; U-test used because of nonnormal distribution; scale not comparable to Figure S2B).

(E) BrdU labeling indices of untransfected (white) or $GFP^+/RFPnls^+$-targeted (gray) cells 48 hr after electroporation at E13.5 with 4D-shRNAs and 3 or 9 hr BrdU exposure.

(F) 9 hr neuronal birthdating calculated as proportion of $GFP^-/RFPnls^-/BrdU^+$ (white) or $GFP^+/RFPnls^+/BrdU^+$ cells in the IZ relative to all $GFP^-/RFPnls^-$ or $GFP^+/RFPnls^+$ progenitors present in the same cortical region of embryos treated as in (E).

(G) Percentage of APs, BPs in the VZ (BP^{VZ}), or BPs in the SVZ (BP^{SVZ}) 48 hr after coelectroporation at E13.5 with control (white), 4D (black), or 4D-shRNA (gray) plasmids. Note the converse effect of RNAi as compared to overexpression.

(E, F, and G) $n \geq 3$; error bars indicate SD; $^*p < 0.05$.

contributed to an almost 3-fold wider cortical surface area at P0 than progenitors transfected with control plasmids, which suggests increased cortical expansion.

This conclusion was corroborated by immunohistochemistry for a neuronal marker of late-born upper layer II-IV, neurons, Brn-2 (Figures 7D and 7E; McEvilly et al., 2002), which showed at P0 an increase by almost 30% in the proportion of $Brn\text{-}2^+$ neurons within the $RFPnls^+$ population upon electroporation with 4D at E13.5 as compared to control plasmids (61.6% ± 5.5% versus 78.1% ± 3.1%) (Figure 7F). Importantly, the distribution of $Brn\text{-}2^+/RFPnls^+$ cells in the ventricular-to-pial axis of the CP was essentially identical upon electroporation with control or 4D plasmids (data not shown), suggesting that the observed effect on expansion of $RFPnls^+$ cortical surface area is not due to an altered migration of neurons.

DISCUSSION

We showed that 4D overexpression in neural progenitors of the developing mouse brain shortens G1, inhibits neurogenesis, and increases the generation and expansion of BPs whereas 4D RNAi induces the opposite effects. Three aspects of our work deserve particular attention.

First, this is to our knowledge the first manipulation of G1 length by a cdk/cyclin complex in vertebrates, because similar manipulations in whole animals have been reported only in flies.

Consistent with our results, overexpression of cdk/cyclin complexes in *Drosophila* can accelerate G1 or G2 while inducing a compensatory lengthening of the other respective phase of the cell cycle (Reis and Edgar, 2004). It should be noticed, however, that in our experiments a shorter G1 was more likely achieved by

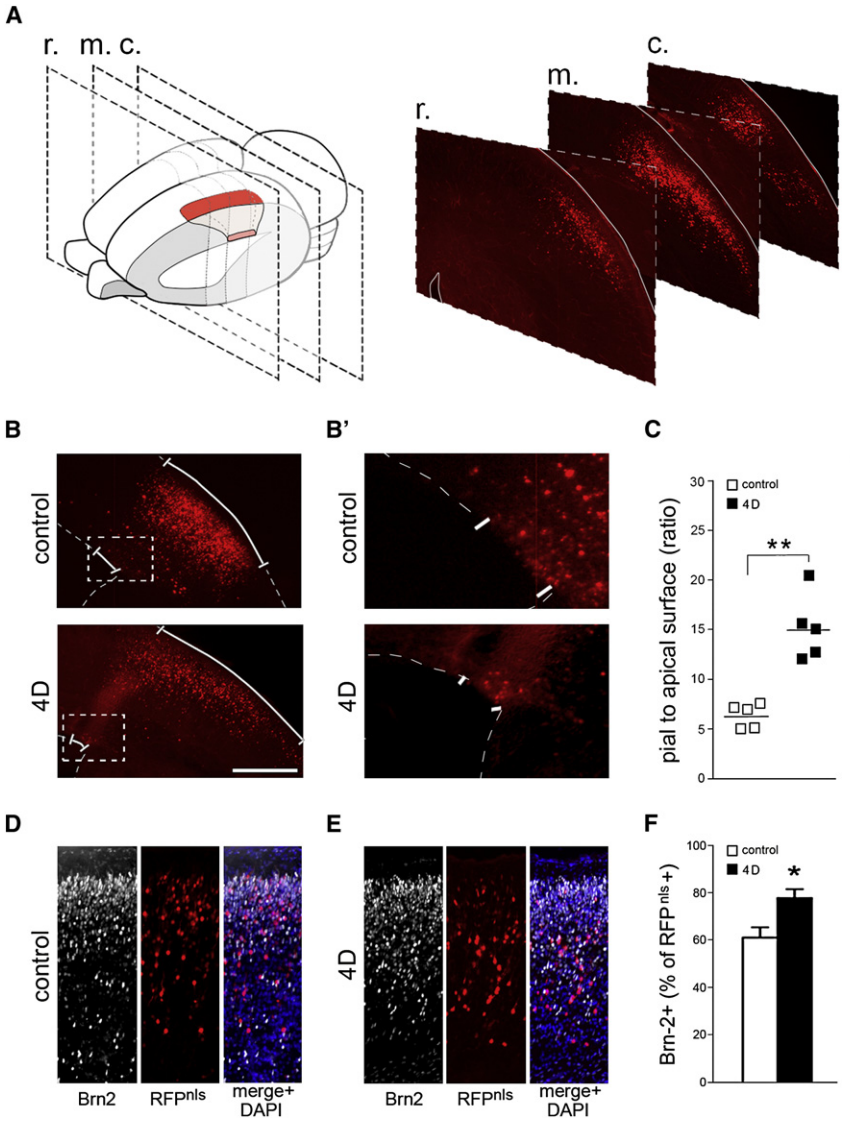

Figure 7. 4D Overexpression Increases RFPnls$^+$ Pial-to-Apical Surface Area at P0

(A) Representation of the analyses performed at P0 after serial sectioning through the RFPnls$^+$ area (red area; left) and examples of fluorescence fields at its rostral (r.), medial (m.), or caudal (c.) portion (right) used to 3D-reconstruct the volume containing red fluorescence.

(B) Fluorescence pictures of 50-μm-thick vibratome sections after targeting with control (top) or 4D (bottom) plasmids at E13.5 (line indicates portion containing RFPnls$^+$ cells; dashed line indicates cortical boundaries); scale bar represents 500 μm.

(B′) Magnification of the dashed box in (B) showing the apical portion of the VZ being judged to contain RFPnls$^+$ cells (space between white lines).

(C) Ratio of pial-to-apical surface area after electroporation with control (white) or 4D (black) plasmids. Each symbol represents quantification of an individual brain from at least three litters (horizontal lines indicate mean).

(D and E) Fluorescence pictures of the P0 CP after electroporation at E13.5 with either control (D) or 4D (E) plasmids and Brn-2 immunostaining.

(F) Proportion of Brn-2$^+$/RFPnls$^+$ cells as in (D) (white) or (E) (black), respectively (error bars indicate SD).

*$p < 0.05$; **$p < 0.005$.

preventing its physiological lengthening, rather than by accelerating it. This is supported by the fact that (1) overexpressed 4D was more effective on Tis21$^+$ progenitors, which lengthen G1 more than Tis21$^-$ progenitors (Calegari et al., 2005) and (2) the G1 of E14.5 4D-transfected cells was essentially identical to that of E13.5 progenitors (Takahashi et al., 1995) (Table S1). In essence, high levels of 4D may just have prevented the lengthening of G1 normally occurring from E13.5 to E14.5, instead of accelerating G1 at E14.5. Moreover, 4D overexpression in flies has been found to increase cell size, and a similar effect by its human ortholog has been taken as evidence for a growth-specific function of 4D that is conserved from arthropods to mammals (Datar et al., 2006). However, overexpression of mouse 4D did not increase, nor decrease, the size of mouse neural progenitors, which may add new insights into the long-debated relationship between cell growth and cell cycle progression of mammalian cells (Jorgensen and Tyers, 2004; Tapon et al., 2001).

Second, shortening the G1 of neural progenitors inhibited the switch from proliferation to differentiation whereas lengthening G1 promoted it.

In line with our data, previous studies on trophic factors have shown a correlation between faster cell cycles and a delay of neurogenesis (Hodge et al., 2004; Lukaszewicz et al., 2002; Maric et al., 2007). However, in these studies, it has been difficult to conclude that cell cycle length had a direct causal role on differentiation because of the multiple and complex effects triggered by the factors themselves. In this context, cyclinD1 alone has also been found to bind in a cdk-independent manner several transcription factors and transcriptional coregulators, which may influence differentiation (Fu et al., 2004). However, such cell-cycle-independent roles of cyclinD1 on differentiation of neural progenitors can here be excluded because electroporation of cyclinD1 alone was less, rather than more, effective in inhibiting neurogenesis than electroporation of 4D (data not shown).

Importantly, inhibition of neurogenesis by overexpression of 4D was accompanied by an increased proportion of BPs in the VZ without any change in the proportion of APs. If we consider that APs generate BPs by asymmetric division (Haubensak et al., 2004; Miyata et al., 2004; Noctor et al., 2004), and if we exclude the possibility that 4D may induce a change from asymmetric to symmetric division, which is supported by our analysis of cleavage plane angle of mitotic APs, our data are consistent with a model in which a shorter G1 induces neurogenic APs to

undergo asymmetric division that generates one AP and one BP instead of one AP and one neuron with, in addition, a higher proportion of BPs remaining (or becoming) proliferative (Figure S5), thereby increasing the thickness of the SVZ.

Because the only reported function of 4D in vertebrates is to control G1 progression, we conclude that a shorter G1 is the primary cause of the inhibition of neurogenesis and increased proliferation of neural progenitors. Consistent with this conclusion, 4D overexpression in proliferating APs did not change their fate as these progenitors already have, in relative terms, the shortest G1 (Calegari et al., 2005) and the highest proliferative potential. Conversely, a pharmacological lengthening of G1 of proliferating APs was shown to induce their premature switch to neurogenesis (Calegari and Huttner, 2003), and similarly, 4D knockdown by RNAi lengthened G1, increased neurogenesis, and decreased the proportion of BPs. Thus, we conclude that lengthening of G1 is both necessary and sufficient to induce the switch of neural progenitors from proliferation to neurogenesis and, as such, should be considered as a primary cause, and not a consequence, of neurogenesis.

Third, a higher proportion of BPs during development correlated at birth with an increased cortical surface area contributed by 4D-targeted progenitors.

Specifically, we found that a 40% increase in the proportion of BPs 24 hr after electroporation with 4D was followed by a similar increase in SVZ thickness the subsequent day (with less than half of all BPs being transfected) and at P0 by a 3-fold increase in the pial-to-apical surface area containing RFPnls$^+$ neurons. This is fundamentally different from the effect of β-catenin in APs (Chenn and Walsh, 2002), which induces expansion of APs but not BPs leading to decreased, rather than increased, pial-to-apical surface area.

It may seem paradoxical that inhibition of neurogenesis leads to an increased cortical surface area. However, electroporation is a transient transfection system in which plasmids are exponentially diluted as a result of cell division leading, in particular for gene products with a very short half-life such as cyclins, to the rapid termination of the overexpression effect. For example, with a cell cycle of 14 hr, 4D plasmids electroporated at E13.5 will be diluted at E15.5 by more than a 10-fold factor, likely sufficient to allow progenitors to resume physiological corticogenesis. However, because of the increased progenitor expansion between E13.5 and E15.5, neuronal output will ultimately also increase.

We find it unlikely that 4D overexpression may influence neuronal migration because the distribution of upper layer II-IV Brn-2$^+$ neurons at P0 was essentially identical to that of controls. Therefore, the wider cortical surface area containing neurons derived from 4D-targeted progenitors, together with the increased proportion of Brn-2$^+$ neurons, strongly suggests that an increase in BPs during development can cause cortical expansion. This, importantly, is fully consistent with the hypothesis that an increased proportion of BPs in higher mammals is a principal cause for cortical expansion during evolution (Abdel-Mannan et al., 2008; Fish et al., 2008; Kriegstein et al., 2006; Pontious et al., 2008). Thus, our study may provide the first experimental evidence for a manipulation of BP expansion in support to their suggested role in evolution.

In conclusion, our work contributes novel data for better understanding cell cycle control, expansion versus differentiation of neural stem and progenitor cells, and perhaps, regulation of brain size in a developmental and evolutionary perspective. Finally, we find it likely that time (G1 length) may have a similar role in controlling the expansion versus differentiation of adult neural and perhaps any other somatic, stem, or progenitor cell, which may be key toward novel approaches of regenerative therapies.

EXPERIMENTAL PROCEDURES

Cloning

Full-length cDNAs of mouse cdk2, cdk4, and cyclinE1 were purchased from the FANTOM consortium (RIKEN, Japan). CyclinD1 was provided by Dr. Charles J. Sherr. Cdks and cyclins were subcloned into pCMS-EGFP (Clontech) or pDSV-mRFPnls (De Pietri Tonelli et al., 2006), respectively. Plasmids encoding D- or 4-shRNA were kindly provided by Dr. Pumin Zhang or purchased from SA-Biosciences, respectively (details in Supplemental Data).

In Utero Electroporation

In utero electroporation was performed as previously described (De Pietri Tonelli et al., 2006). In brief, C57BL/6J mice (defined as 0.5 day of gestation the morning of vaginal plug) were anesthetized with isofluorane and their uteri exposed. Via a glass capillary, 1–3 μl of PBS containing 1–3 μg/μl of plasmids were injected into the lumen of the embryonic telencephalon, and 6 pulses of 30 V, 50 ms each at 1 s intervals were delivered through platinum electrodes (1 mm diameter) with a BTX-830 electroporator (Genetronics). The uterus was then relocated into the peritoneal cavity and the abdomen sutured. Mice, eventually subjected to BrdU(/EdU) injection, were allowed to complete gestation or sacrificed at different times after surgery to collect embryos.

S Phase Labeling

Cumulative BrdU labeling was carried out by repeated intraperitoneal injections of 1 mg BrdU (Sigma) at 3 hr intervals for a total of 2, 3, 6, 9, or 12 hr. For determination of S phase entry or exit, BrdU injection was followed after 45 min by injection of 0.1 mg EdU (Invitrogen) and sacrifice 45 min later.

Microscopy

Brains were analyzed with a fluorescence stereomicroscope (Olympus SXZ16) and those targeted in the lateral cortex were fixed overnight at 4°C in 4% PFA followed by equilibration in 30% sucrose and embedding in Tissue-Tek. Immunolabeling on 10 μm thick cryosections was performed after permeabilization with 0.3% Triton X-100, quenching with 0.1 M glycine-Tris (pH 7.4) and, eventually, treatment with 2 M HCl for BrdU detection (see Supplemental Data and Table S2 for antibodies and conditions). EdU was detected according to manufacturer's instructions (Invitrogen). Sections were analyzed with a conventional (Olympus BX61) or confocal (Zeiss LSM510 Axiovert 200M) fluorescence microscope as indicated in figure legends. Images were acquired with IP Lab 4.0 (BD Biosciences) or ZEISS LSM 4.2 (Carl Zeiss) and processed with ImageJ 1.33 (Wayne Rasband) or Photoshop CS3 (Adobe).

Calculation of Cell Cycle Phases

Calculation was performed within the VZ by nonlinear regression analysis of cumulative and mitotic BrdU labeling indices (Excel spreadsheet kindly provided by Dr. Richard S. Nowakowski) (Takahashi et al., 1995) (1.0 labeling index = 100%). In brief, the intercepts of the best nonlinear fit with the abscissa (y) and the time (z) needed to reach the maximum labeling index (growth fraction = GF) correspond to the (1) length of S (T_S) relative to the cell cycle (T_C) and (2) $T_C - T_S$, respectively, allowing us to solve the equations $\begin{cases} Tc - Ts = z \\ (Ts/Tc)GF = y \end{cases}$. Length of G2+M corresponded to the time required to label all mitotic cells.

Determination of Pial-to-Apical Surface Area

P0 brains were fixed, embedded in 3% low-melting agarose, and cut through the rostral-to-caudal axis in 50-μm-thick sections with a vibratome Leica VT1200 (Leica). Sections were analyzed with a fluorescence stereomicroscope (Olympus SXZ16) and length of pial and apical surfaces containing RFPnls$^+$ cells was measured with the Olympus Cell* program. Pial and apical

surface areas were calculated as the sum of the lengths of each section (in total 20–40) times its thickness.

Statistical Analysis

Statistical analyses were performed by pulling together the counts from 1–4 cryosections or brains (>200 cells total), considering at least 3 litters for calculation of mean and standard deviation. Significance was evaluated by Student's t test.

SUPPLEMENTAL DATA

Supplemental Data include Supplemental Results and Discussion, Supplemental Experimental Procedures, five figures, and two tables and can be found with this article online at http://www.cell.com/cell-stem-cell/supplemental/S1934-5909(09)00284-7.

ACKNOWLEDGMENTS

We thank Dr. Charles J. Sherr and Dr. Pumin Zhang for cyclinD1 and cyclinD1-shRNA plasmids, respectively; Ina Nüsslein, Christiane Rubbert, and the staff of the MPI-CBG animal house for excellent support; and Jeremy N. Pulvers for discussions. Animal experiments were approved by local authorities (249168.11-9-2007-1/2). C.L. and F.C. were supported by the DFG-funded Center for Regenerative Therapies and Medical Faculty of the Technical University, Dresden. Authors' contribution is as follows (C.L.-W.B.H.-F.C.): planning experiments 30%-5%-65%; performing experiments 95%-0%-5%; data analyses 45%-5%-50%, preparation of the manuscript 15%-5%-80%. Authors have no financial interest related to this work.

Received: January 12, 2009
Revised: April 23, 2009
Accepted: May 29, 2009
Published: September 3, 2009

REFERENCES

Abdel-Mannan, O., Cheung, A.F., and Molnar, Z. (2008). Evolution of cortical neurogenesis. Brain Res. Bull. *75*, 398–404.

Attardo, A., Calegari, F., Haubensak, W., Wilsch-Brauninger, M., and Huttner, W.B. (2008). Live imaging at the onset of cortical neurogenesis reveals differential appearance of the neuronal phenotype in apical versus basal progenitor progeny. PLoS ONE *3*, e2388.

Bally-Cuif, L., and Hammerschmidt, M. (2003). Induction and patterning of neuronal development, and its connection to cell cycle control. Curr. Opin. Neurobiol. *13*, 16–25.

Calegari, F., and Huttner, W.B. (2003). An inhibition of cyclin-dependent kinases that lengthens, but does not arrest, neuroepithelial cell cycle induces premature neurogenesis. J. Cell Sci. *116*, 4947–4955.

Calegari, F., Marzesco, A.M., Kittler, R., Buchholz, F., and Huttner, W.B. (2004). Tissue-specific RNA interference in post-implantation mouse embryos using directional electroporation and whole embryo culture. Differentiation *72*, 92–102.

Calegari, F., Haubensak, W., Haffner, C., and Huttner, W.B. (2005). Selective lengthening of the cell cycle in the neurogenic subpopulation of neural progenitor cells during mouse brain development. J. Neurosci. *25*, 6533–6538.

Canzoniere, D., Farioli-Vecchioli, S., Conti, F., Ciotti, M.T., Tata, A.M., Augusti-Tocco, G., Mattei, E., Lakshmana, M.K., Krizhanovsky, V., Reeves, S.A., et al. (2004). Dual control of neurogenesis by PC3 through cell cycle inhibition and induction of Math1. J. Neurosci. *24*, 3355–3369.

Caviness, V.S., Jr., Takahashi, T., and Nowakowski, R.S. (1995). Numbers, time and neocortical neuronogenesis: A general developmental and evolutionary model. Trends Neurosci. *18*, 379–383.

Chenn, A., and Walsh, C.A. (2002). Regulation of cerebral cortical size by control of cell cycle exit in neural precursors. Science *297*, 365–369.

Datar, S.A., Galloni, M., de la Cruz, A., Marti, M., Edgar, B.A., and Frei, C. (2006). Mammalian cyclin D1/Cdk4 complexes induce cell growth in *Drosophila*. Cell Cycle *5*, 647–652.

De Pietri Tonelli, D., Calegari, F., Fei, J.F., Nomura, T., Osumi, N., Heisenberg, C.P., and Huttner, W.B. (2006). Single-cell detection of microRNAs in developing vertebrate embryos after acute administration of a dual-fluorescence reporter/sensor plasmid. Biotechniques *41*, 727–732.

Dehay, C., and Kennedy, H. (2007). Cell-cycle control and cortical development. Nat. Rev. Neurosci. *8*, 438–450.

Ekholm, S.V., and Reed, S.I. (2000). Regulation of G(1) cyclin-dependent kinases in the mammalian cell cycle. Curr. Opin. Cell Biol. *12*, 676–684.

Englund, C., Fink, A., Lau, C., Pham, D., Daza, R.A., Bulfone, A., Kowalczyk, T., and Hevner, R.F. (2005). Pax6, Tbr2, and Tbr1 are expressed sequentially by radial glia, intermediate progenitor cells, and postmitotic neurons in developing neocortex. J. Neurosci. *25*, 247–251.

Fish, J.L., Dehay, C., Kennedy, H., and Huttner, W.B. (2008). Making bigger brains—The evolution of neural-progenitor-cell division. J. Cell Sci. *121*, 2783–2793.

Fu, M., Wang, C., Li, Z., Sakamaki, T., and Pestell, R.G. (2004). Minireview: Cyclin D1: Normal and abnormal functions. Endocrinology *45*, 5439–5447.

Georgopoulou, N., Hurel, C., Politis, P.K., Gaitanou, M., Matsas, R., and Thomaidou, D. (2006). BM88 is a dual function molecule inducing cell cycle exit and neuronal differentiation of neuroblastoma cells via cyclin D1 down-regulation and retinoblastoma protein hypophosphorylation. J. Biol. Chem. *281*, 33606–33620.

Götz, M., and Huttner, W.B. (2005). The cell biology of neurogenesis. Nat. Rev. Mol. Cell Biol. *6*, 777–788.

Haubensak, W., Attardo, A., Denk, W., and Huttner, W.B. (2004). Neurons arise in the basal neuroepithelium of the early mammalian telencephalon: A major site of neurogenesis. Proc. Natl. Acad. Sci. USA *101*, 3196–3201.

Hodge, R.D., D'Ercole, A.J., and O'Kusky, J.R. (2004). Insulin-like growth factor-I accelerates the cell cycle by decreasing g1 phase length and increases cell cycle reentry in the embryonic cerebral cortex. J. Neurosci. *24*, 10201–10210.

Iacopetti, P., Michelini, M., Stuckmann, I., Oback, B., Aaku-Saraste, E., and Huttner, W.B. (1999). Expression of the antiproliferative gene TIS21 at the onset of neurogenesis identifies single neuroepithelial cells that switch from proliferative to neuron-generating division. Proc. Natl. Acad. Sci. USA *96*, 4639–4644.

Jorgensen, P., and Tyers, M. (2004). How cells coordinate growth and division. Curr. Biol. *14*, R1014–R1027.

Kriegstein, A., Noctor, S., and Martinez-Cerdeno, V. (2006). Patterns of neural stem and progenitor cell division may underlie evolutionary cortical expansion. Nat. Rev. Neurosci. *7*, 883–890.

Lukaszewicz, A., Savatier, P., Cortay, V., Kennedy, H., and Dehay, C. (2002). Contrasting effects of basic fibroblast growth factor and neurotrophin 3 on cell cycle kinetics of mouse cortical stem cells. J. Neurosci. *22*, 6610–6622.

Lukaszewicz, A., Savatier, P., Cortay, V., Giroud, P., Huissoud, C., Berland, M., Kennedy, H., and Dehay, C. (2005). G1 phase regulation, area-specific cell cycle control, and cytoarchitectonics in the primate cortex. Neuron *47*, 353–364.

Maric, D., Fiorio Pla, A., Chang, Y.H., and Barker, J.L. (2007). Self-renewing and differentiating properties of cortical neural stem cells are selectively regulated by basic fibroblast growth factor (FGF) signaling via specific FGF receptors. J. Neurosci. *27*, 1836–1852.

McConnell, S.K. (1995). Constructing the cerebral cortex: neurogenesis and fate determination. Neuron *15*, 761–768.

McEvilly, R.J., de Diaz, M.O., Schonemann, M.D., Hooshmand, F., and Rosenfeld, M.G. (2002). Transcriptional regulation of cortical neuron migration by POU domain factors. Science *295*, 1528–1532.

Miyata, T., Kawaguchi, A., Saito, K., Kawano, M., Muto, T., and Ogawa, M. (2004). Asymmetric production of surface-dividing and non-surface-dividing cortical progenitor cells. Development *131*, 3133–3145.

Nguyen, L., Besson, A., Heng, J.I., Schuurmans, C., Teboul, L., Parras, C., Philpott, A., Roberts, J.M., and Guillemot, F. (2006). p27kip1 independently promotes neuronal differentiation and migration in the cerebral cortex. Genes Dev. *20*, 1511–1524.

Noctor, S.C., Martinez-Cerdeno, V., Ivic, L., and Kriegstein, A.R. (2004). Cortical neurons arise in symmetric and asymmetric division zones and migrate through specific phases. Nat. Neurosci. *7*, 136–144.

Noctor, S.C., Martinez-Cerdeno, V., and Kriegstein, A.R. (2008). Distinct behaviors of neural stem and progenitor cells underlie cortical neurogenesis. J. Comp. Neurol. *508*, 28–44.

Ohnuma, S., and Harris, W.A. (2003). Neurogenesis and the cell cycle. Neuron *40*, 199–208.

Ohnuma, S., Philpott, A., Wang, K., Holt, C.E., and Harris, W.A. (1999). p27Xic1, a Cdk inhibitor, promotes the determination of glial cells in *Xenopus* retina. Cell *99*, 499–510.

Peng, S., York, J.P., and Zhang, P. (2006). A transgenic approach for RNA interference-based genetic screening in mice. Proc. Natl. Acad. Sci. USA *103*, 2252–2256.

Politis, P.K., Makri, G., Thomaidou, D., Geissen, M., Rohrer, H., and Matsas, R. (2007). BM88/CEND1 coordinates cell cycle exit and differentiation of neuronal precursors. Proc. Natl. Acad. Sci. USA *104*, 17861–17866.

Pontious, A., Kowalczyk, T., Englund, C., and Hevner, R.F. (2008). Role of intermediate progenitor cells in cerebral cortex development. Dev. Neurosci. *30*, 24–32.

Popken, G.J., Hodge, R.D., Ye, P., Zhang, J., Ng, W., O'Kusky, J.R., and D'Ercole, A.J. (2004). In vivo effects of insulin-like growth factor-I (IGF-I) on prenatal and early postnatal development of the central nervous system. Eur. J. Neurosci. *19*, 2056–2068.

Rakic, P. (1995). A small step for the cell, a giant leap for mankind: a hypothesis of neocortical expansion during evolution. Trends Neurosci. *18*, 383–388.

Regad, T., Bellodi, C., Nicotera, P., and Salomoni, P. (2009). The tumor suppressor Pml regulates cell fate in the developing neocortex. Nat. Neurosci. *12*, 132–140.

Reis, T., and Edgar, B.A. (2004). Negative regulation of dE2F1 by cyclin-dependent kinases controls cell cycle timing. Cell *117*, 253–264.

Sherr, C.J. (1994). G1 phase progression: Cycling on cue. Cell *79*, 551–555.

Takahashi, T., Nowakowski, R.S., and Caviness, V.S., Jr. (1995). The cell cycle of the pseudostratified ventricular epithelium of the embryonic murine cerebral wall. J. Neurosci. *15*, 6046–6057.

Tapon, N., Moberg, K.H., and Hariharan, I.K. (2001). The coupling of cell growth to the cell cycle. Curr. Opin. Cell Biol. *13*, 731–737.